Article

Not peer-reviewed version

Graphene Oxide Doped CNT Membranes for Dye Adsorption

Mariafrancesca Baratta *, Fiore Pasquale Nicoletta, Giovanni De Filpo *

Posted Date: 15 April 2025

doi: 10.20944/preprints202504.1306.v1

Keywords: water pollutants; carbon nanotubes; buckypapers; graphene oxide; dyes

 doi:10.20944/preprints202504.1306.v1

Article

Graphene Oxide Doped CNT Membranes for Dye Adsorption

Mariafrancesca Baratta [1,*], Fiore P. Nicoletta [2] and Giovanni De Filpo [1,*]

[1] Department of Chemistry and Chemical Technologies, University of Calabria, 87036 Rende – Italy

[2] Department of Pharmacy, Health and Nutritional Sciences, University of Calabria, 87036 Rende – Italy

* Correspondence: mariafrancesca.baratta@unical.it (M.B.); defilpo@unical.it (G.D.F.)

Abstract: Recently, graphene oxide (GO) has been largely investigated as potential adsorbent towards dyes. However, the major obstacle to its fully employment is linked to its natural powder consistence, which greatly complexifies the operations of recovery and reuse. With the aim to overcome this issue, the present work reports the design of GO modified carbon nanotubes buckypapers (BPs), in which the main component, GO, is entirely entrapped in the BP grid generated by CNTs, for the double purpose of a) increasing adsorption performance of GO-BPs and b) ensure a fast process of regeneration and reuse. Adsorption experiments were performed towards several dyes: Acid Blue 29 (AB29), Crystal Violet (CV), Eosyn Y (EY), Malachite Green (MG), and Rhodamine B (RB) (C_i = 50 ppm, pH=6). Results demonstrated that adsorption is strictly dependent on the charge occurring both on GO-BP and dye surfaces, observing great adsorption capacities towards MG (493.44 mg g^{-1}), RB (467.35 mg g^{-1}) and CV (374.53 mg g^{-1}), due to the best coupling of dye cationic form with negative GO-BP surface. Confirmed also by kinetic constants, where higher values are those of MG, RB and CV, the following trend in GO-BP adsorption performance has been derived: MG ≈ RB > CV > AB29 > EY.

Keywords: water pollutants; carbon nanotubes; buckypapers; graphene oxide; dyes

1. Introduction

Together with water scarcity, water pollution represents one of the biggest threats and one of the most difficult challenges of this century. As evidence of this, latest UNO Report on the status of achievement of Sustainable Development Goals contained in the 2030 Agenda states that progress in G6 Goal ("Ensure availability and sustainable management of water and sanitation for all") "remains insufficient, despite some improvements. At the current speed, in 2030, 2 billion people will still live without safely managed drinking water, 3 billion without safely managed sanitation and 1.4 billion without basic hygiene services" [1]. One of the major difficulties in resolving the problem of water pollution is indeed the wide variety and complexity of contaminants ending up in wastewater, making currently wastewater treatment technologies inefficient and more often obsolete. Among the unlimited possibilities of organic and inorganic pollutants found in water, dyes and pigments stand out for their huge amount and diversity. This strong occurrence is the result of application of dyes, both natural or synthetic, in a considerable part of anthropogenic activities, covering a lot of industry sectors, such as paper, leather, food, cosmetic, paint, and, above all, textile. The latter indeed consumes more than 80% of global annual production of synthetic dyes, estimated to be around 800,000 tons per year [2], managing a textile market, according to latest Market Report by IMARC Group, that reached a value of USD 1,065.6 Billion in 2024, and it is expected to increase by an additional 39% by 2033 [3]. Furthermore, most of textile manufacturing operations, such as dyeing, finishing, tinting, sourcing, sizing, de-sizing, printing, are detrimental, since huge volumes of textile waters produced during these processes and containing all dyes not stuck on fabrics are often released into the environment without adequate control [2]. The risk associated with the occurrence of dyes in water includes multiple factors. Generally, dyes are not bio-degradable compounds, with

 doi:10.20944/preprints202504.1306.v1

chemical resistance to heat and light, acting as promotors in discoloration of water bodies [4]. Moreover, due to their ability to absorb and reflect sunlight, the amount of light reaching the photic zone is strongly reduced by dyestuff occurrence, causing an interference in the natural photosynthetic activity of aquatic flora [5]. Thirdly, it has been demonstrated that dyes can have a mutagenic and carcinogenic potential towards human health, leading to the development of diseases such skin and eye irritation, dermatitis, ovulation and spermatogenesis interference, problems to the central nervous system, and carcinogenesis [2,6,7]. In this tragic scenario, a prompt action aimed at changing the course of events is extremely required.

Currently, treatment of dyestuff wastewater involves the employment of different technologies, both physical such as sedimentation, and adsorption, chemical like flocculation, photodegradation, chemical oxidation, and electrochemical treatments, and biological [8–12]. With a lot of advantages in terms of process feasibility, large recovery percentages and eco-friendliness, adsorption represents above all an indispensable tool in the treatment of textile water [13,14]. Along these lines, adsorption can further count on a wide range of nanomaterials of recent development, whose large surface area strongly contribute to increase process recovery performance [15]. This includes TiO2 nanoparticles, silicates, resins, MoS2 nanosheets, porous polymers, and carbon-based materials such carbon nanotubes (CNTs), activated carbon, graphene, and graphene oxide (GO) [15–18]. Speaking about the latter, GO turned out to be an excellent candidate for the removal of dyes from wastewater. Its high surface area and flat morphology, resembling a 2D honeycomb structure, fit perfectly with the planarity of most of dyes, originated by the intensive number of aromatic rings in their structures, thus favoring the instauration of hydrophobic interactions with which dyes can be recovered. Furthermore, GO chemical tunability, due to the presence of -OH and -COOH polar functional groups, can enhance and reinforce dyes adsorption through the additional establishment of electrostatic interactions, this way contributing to accelerate and improve the entire process [19]. However, two of the major drawbacks associated with the employment of GO in aqueous solutions are related to the aggregation phenomenon of GO flakes, which reduces consistently the availability of surface area for adsorption, and the nanometric dimensions of particles, which make hard adsorbent recovery, unless additional steps of centrifugation and filtration are performed, and its reuse.

On the other hand, carbon nanotubes, also possessing a large surface area which makes them excellent adsorbents too, differ from GO substantially for their tubular structure. Thanks to this and to their high mechanical properties, CNTs can be opportunely handled in buckypaper (BPs) membranes, entirely made of carbon nanotubes, developing a new “system”, contemporaneously benefiting from the advantages coming from CNTs (chemical stability, electrical conductivity, large surface area) with those of a membrane (porosity, self-standing ability) [16,20,21]. In addition, the preparation of BPs through vacuum assisted filtration can count on a fast, simple and environmentally friendly procedure, by dispersing CNTs in eco-friendly solvents, like methanol or water, which can be recovered at the end of each step of filtration, and reused. Recent developments in this field have shown that BP adsorption properties can be further improved through the incorporation of porous adsorbents, exhibiting large surface area, such as metal organic frameworks (MOFs) [22,23]. In this case, the incorporation of powder dopants into BPs is functional to increase adsorption capacity as much as to avoid recovery problem, due to BP standing-alone properties, facilitating the entire process in terms of recycle and regeneration [24].

Starting from these premises, the aim of the present work is focused on the preparation of GO-buckypaper membranes (GO-BPs), enriched through the entrapment of large amounts of GO (75% w/w), in order to exploit great adsorption potential of GO towards dyes without renouncing to mechanical stability and self-standing ability of BPs, able to ensure an efficient and fast possibility of regeneration and reuse of pristine adsorbents. Five different dyes have been investigated in order to evaluate GO-BPs performance also in terms of selectivity, showing that chemical tunability of GO is the key factor in the adsorption of these pollutants.

 doi:10.20944/preprints202504.1306.v1

2. Materials and Methods

2.1. Materials and Reagents

SWCNTs-COOH (average D = 4-5 nm, L = 0.5-1.5 μm, bundle dimensions) and graphene oxide GO (15–20 sheets, 4–10% edge-oxidized) were both purchased from Sigma-Aldrich, Milan, Italy. Acid Blue 29 (AB29), Crystal Violet (CV), Eosyn Y (EY), Malachite Green (MG), and Rhodamine B (RB) were also purchased from Sigma-Aldrich, Milan, Italy. All chemicals were used as received.

2.2. Buckypaper (GO-BP) Preparation

Preparation of GO buckypaper membranes (GO-BPs) has been carried out referring to wet method technique, following a procedure similarly reported in our previous work [25]. 12.5 mg of SWCNTs-COOH were dispersed in 150 mL of methanol with 37.5 mg of graphene oxide, GO (GO:SWCNTs-COOH: 75:25 w/w%). After sonication (4 h) in an ultrasonic bath (model M1800H-E, Bransonic, Danbury, CT, USA), GO/SWCNTs-COOH dispersions were filtered under vacuum (-0.04 bar, pressure) through PTFE disks (diameter: 47 mm, average pore size: 0.5 μm, Durapore©, Merck KGaA, Darmstadt, Germany). At the end of filtration, after drying at room temperature, GO-BP membranes were peeled from PTFE disks (average D: 35 ± 2 mm, t: 65 ± 1 μm).

2.3. Batch Studies for Dyes Adsorption

Adsorption experiments were conducted by placing 1 GO-BP disk (50 mg) in 100 mL of dye aqueous solutions at initial contaminant concentration of 50 mg L^{-1} for each pollutant. All experiments were performed under stirring (180 rpm) by using an orbital shaker (PSU-10i, Biosan, Italy) and adsorption was evaluated for 48 h at pH=6 and room temperature. The amount of adsorbed dye onto GO-BP membranes is calculated in terms of removal efficiency (RE%) by using Eq. (1):

$$RE\% = \frac{(C_0 - C_e)\cdot 100}{C_0} \qquad (1)$$

where C_0 and C_e represent the initial and at equilibrium concentrations, respectively.

2.4. Characterizations

Scanning electron microscopy (Leica LEO 420, Leica Microsystems, Cambridge, England) was used to elucidate the morphology of GO-BP membranes. Samples were covered with an ultrathin Au layer (10 nm) before investigation, by using Auto Sputter Coater (Agar), and analysis was performed at the following conditions: accelerating voltage of 10 kV, vacuum conditions of $1 \cdot 10^{-6}$ Torr. Mechanical strength of GO-BP membranes was determined with a Sauter TVO-S tensile tester, equipped with a Sauter FH-1k digital dynamometer and AFH FAST software (Sauter GmbH, Balingen, Germany). Rectangular strips (*l x w* = 3 cm x 5 mm) were obtained from GO-BP membranes, tested for elongation measurements at a strain rate of 0.1 mm·min^{-1}. Contact angle measurements were performed at 25°C in static conditions by using a goniometer (Nordtest, Serravalle Scrivia AL, Italy). A drop (2 μL) of water was deposited on sample surface and contact angle values were obtained through the average of set tangents measurements on both droplet visible edges picked up on five different positions of each sample. A zeta potential analyzer (SurPASS TM 3, Anton Paar Italia S.R.L., Turin, Italy, equipped with an adjustable gap cell) was employed to measure the surface charge of GO-BPs as a function of pH value (pH range = 3-9, T = 25°C). After being mounted on sample holders, a pair of each membrane (cross section: 2x1 cm^2) was subjected to changes in pH, by adding 0.05 M of HCl. Z potential was finally calculated from streaming potential measurements through Helmholtz and Smoluchowski equation [26]. Dyes concentration was determined through absorbance measurements on an Evolution 201 spectrophotometer (ThermoFisher Scientific, Hillsboro, OR, USA), equipped with 1.0 cm quartz cells, by using calibration curves of investigated pollutants. Absorbance values were collected in correspondence of λmax of each pollutant, being 602 nm for AB29, 590 nm for CV, 518 nm for EY, 620 nm for MG and 542 nm for RB.

 doi:10.20944/preprints202504.1306.v1

3. Results

3.1. GO-BPs Characterization

GO-BP membranes were prepared by vacuum assisted filtration of GO/SWCNTs-COOH initial mixture. The amount of GO to be incorporated in the neat BP membrane has been previously studied by the authors [25], finding that the optimal ratio GO:SWCNTs-COOH is 75:25 ww%. This choice provides the maximum amount of graphene oxide in the membrane, which is highly adsorptive for dyes due to its planar structure, and, at the same time, the preservation of BP standing-alone properties, facilitating its removal at the end of adsorption process. Furthermore, adopting a technique such as wet method, together with the ease of operation, great advantages come from the use of low amounts of an ecofriendly solvent (methanol) and from the absence of post-synthetic treatments. Despite the huge concentration of graphene oxide, GO-BP membranes maintain the typical texture of BPs, where CNTs filaments are braided between themselves, due to π−π and van der Waals interactions, forming an entangled net. Along the outer surface of CNTs bundles, GO sheets are positioned, where π−π and van der Waals interactions between the flat surface of GO and the round one of CNTs keep GO flakes incorporated and homogeneously disposed inside the membrane (Figure 1). Thanks to this high number of interactions, GO-BPs exhibit a noticeable mechanical stability, confirmed by tensile strength measurements performed on them. Young modulus of as-obtained membranes is found to be 0.7 ± 0.1 GPa, with a tensile strength value of ~ 5 MPa (Figure 2b). It is worth to note that the inclusion of graphene oxide into a BP membrane inevitably change mechanical properties of pure BPs. These last are entirely made of carbon nanotubes, which can support and strengthen the membrane network through their long tubular structure. In contrast, in GO-BPs, 75% of CNTs amount is totally replaced by graphene oxide, which cannot cover the role of missing CNTs with its flat and planar morphology. Therefore, as expected, mechanical stability of GO-BPs is slightly lowered than neat BPs, whose Young modulus is typically around 0.9 GPa. Anyway, on a larger scale based on more materials than only buckypapers, GO-BP tensile strength is still high, ensuring a great mechanical stability for the purpose of this work. Due to their chemical composition, made of carboxylic and hydroxylic groups, it is supposed that GO doped buckypapers are hydrophilic. Contact angle measurements clearly confirm this character, with a CA value equal to 40.7° ± 0.5°. GO-BP surface charge, in terms of Z potential, as a function of pH is reported in Figure 2a. As shown in figure, the point of zero charge (pH_{ZCP}), i.e. the pH value at which net surface charge is 0, is 4.4. Consequently, when $pH < pH_{ZCP}$, GO-BP surface is positive with -COOH and -OH groups in their acid form; otherwise, if $pH > pH_{ZCP}$, carboxylic and hydroxylic groups start deprotonation and GO-BP surface becomes more negative with increasing pH.

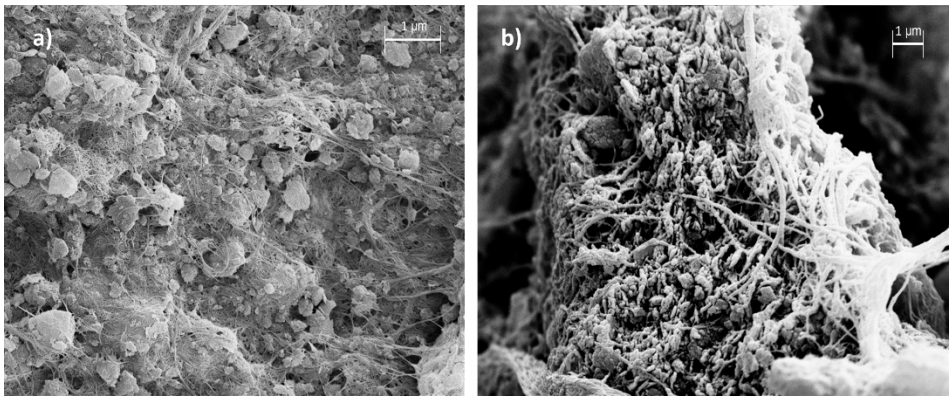

Figure 1. SEM images of (a) GO-BP surface and (b) GO-BP cross section.

 doi:10.20944/preprints202504.1306.v1

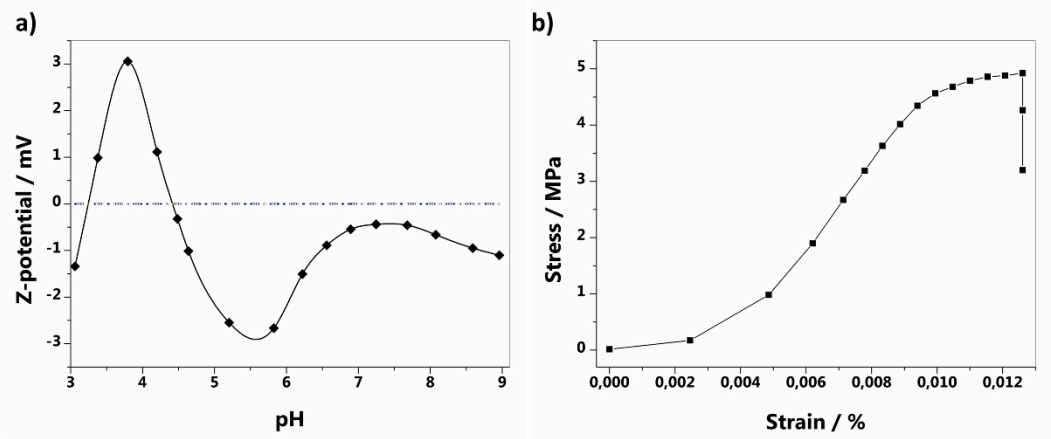

Figure 2. (a) Z-potential of GO-BPs. (b) Stress vs strain curve of GO-BPs.

3.2. Dyes Adsorption

GO-BP membranes were projected for dyes adsorption from aqueous solutions. To investigate their adsorptive properties, five different pollutants were chosen, according to reasons related to natural chemical composition, in order to cover different classes of dyes, and wastewater abundance. Starting from this premise, the following dyes were selected: Acid Blue 29 (AB29, an anionic disazo dye), Crystal Violet (CV, a a triarylmethane dye), Eosyn Y (EY, a triarylmethane dye), Malachite Green (MG, a triarylmethane dye), and Rhodamine B (RB, a xanthene dye). The incorporation of graphene oxide into BP membranes is functional to the enhancement of BP capture properties without renouncing to their self-standing ability. Literature works clearly show that high recovery percentages can be obtained when graphene oxide is employed as an adsorbent [27,28]. This can be ascribed to the extraordinary compatibility between GO flat morphology and chemical planar structure of majority of dyes, which allows to maximize the number of interactions among the two parties involved, thus favoring their adsorption. Furthermore, the option to toggle the charge on GO surface, alternating between a neutral or charged form simply depending on pH, reinforces dyes adsorption through the additional establishment of electrostatic interactions, being lot of dyes cationic or anionic in chemical nature [29–31]. The employment of GO in the form of powder brings some difficulties during the adsorbent recovery phase, due to its nanosized dimensions. As a result, just to overcome this problematic, in the present work, GO has been incorporated in buckypaper membranes, preparing an alternative BP version which aims to combine high adsorption properties of GO, enhancing those already held by pristine BPs, with their mechanical stability and self-standing ability.

Adsorption experiments were performed in batch, at room temperature, and at pH=6 in order to simulate a condition similar as much as possible to that of dyes in wastewater. One GO-BP disk was employed each 100 mL of pollutant solution, previously prepared at initial concentration value of 50 mg L^{-1}. Capture properties of GO-BP were evaluated for a period of 48 h, by taking samples at cadenced intervals of 5 min and monitoring the decrease in dye concentration through UV-Vis spectroscopy, set at λ_{max} of each pollutant. Figure 3a reports the adsorption of AB29, CV, EY, MG, and RB by GO-BPs after a period of 48 h. Adsorption curves clearly indicate that, to parity of initial concentration (50 mg L^{-1}), GO-BP capture properties differ quite enough among dyes, with RB and MG showing the highest values of recovery (Figure 3b, RE_{RB} = 94.5%, RE_{MG} = 95.5%). In fact, comparing curves of Figure 3a, it comes out that, after 8 h, CV, MG and RB have already halved their initial concentration, attaining values of 27.1, 22.6 and 18.3 mg L^{-1} respectively, while EY and AB29 remain a long way off from 25 ppm, moving instead towards the equilibrium values. Furthermore, concentrations of CV, MG and RB drop quite abruptly of an ulterior 30% in the remaining time before 24 h, after which adsorption equilibrium is reached. In fact, after 24 h, only a slightly increase in RE% (~5%) is observed up to 48 h, exception for EY, which instead achieves equilibrium at t = 240 min.

 doi:10.20944/preprints202504.1306.v1

These differences in adsorption behavior of dyes are ascribable to chemical interactions establishing between GO-BP membrane and the investigated pollutant. Typical interactions involved during adsorption include π-π, Van der Waals and electrostatic interactions. At pH=6, at which experiments are performed, GO-BP surface is negatively charged. On the other hand, depending on their pK_a values, dyes molecules could exhibit a neutral or charged form. In particular, at pH = 6, CV ($pK_{a1} \approx 1.15$ and $pK_{a2} \approx 1.8$), rapidly losing two protons in acidic conditions, maintains a positive charge on one in three nitrogens of its chemical structure while MG ($pK_a \approx 6.9$) is doubly protoned on its N atoms. RB ($pK_a \approx 4.8$), instead, due to the presence of a carboxylate group, exhibits a neutral form. Finally, EY ($pK_a \approx 4.8$) and AB29, in consequence of the presence on their structures of a carboxylate and two sulfonic groups respectively, are both negatively charged. Starting from these premises, electrostatic interactions play a pivotal role in the adsorption of investigated dyes on GO-BP membranes (Figure 4) [27,32]. In fact, as shown in Figure 3b, lowest adsorption values are observed for EY and AB29, where adsorption phenomenon, torn between two conflicting forces, suffers prevalently from electrostatic repulsion between dye and membrane surface (both negatively charged), despite the positive tendency to recovery due to π-π and Van der Waals interactions. Contrariwise, in the case of CV, MB and RB, both forces, electrostatic and hydrophobic, point in the same direction since aromatic structure of investigated dyes suits perfectly with flat morphology of GO-BPs, and adsorption is strongly assisted by electrostatic attraction among positive dyes and negative charge on membrane surface. Furthermore, it could be observed that the highest charged quantity (MG), the highest recovery value, suggesting the importance of electrostatic interactions in this process. This behavior, leading to a preferential adsorption of cationic dyes on GO surface owed to electrostatic attraction, has been already evidenced by Ramesha et al. [32]. The authors reported the difference of GO adsorption performance towards cationic and anionic dyes, concluding that the formers were better retained on graphene oxide thanks to the primary role covered by charge-based interactions.

Considering the adsorption capacity of GO-BP membranes at 50 mg L^{-1}, the following trend can be derived: MG (390.17 mg g^{-1}) ≈ RB > CV > AB29 > EY (67.09 mg g^{-1}). All q_{max} values are reported in Table 1. Further evidence comes from the calculation of dye distribution coefficient (Eq. 2), K_D, on GO-BP membrane [33]:

$$K_D = \frac{[dye]_{GO-BP}}{[dye]_{sol}} \quad (2)$$

with $[dye]_{GO-BP}$ (mg Kg^{-1}) and $[dye]_{sol}$ (mg L^{-1}) being equilibrium dye concentrations adsorbed on GO-BP membrane and in solution, respectively. Generally, when $\log K_D > 5$, high affinity between adsorbent and adsorbate substists. $LogK_D$ values for AB29, EY, CV, MG and RB are reported in Table 1. As expected, high affinity is observed when the pollutants are MG and RB ($logK_{MG} = 5.23$ and $logK_{RB} = 5.14$), confirming the greatest percentages of adsorption recovery on GO-BP membranes, followed by CV ($logK_{CV} = 4.50$), AB29 ($logK_{AB29} = 3.58$), and EY ($logK_{EY} = 3.21$).

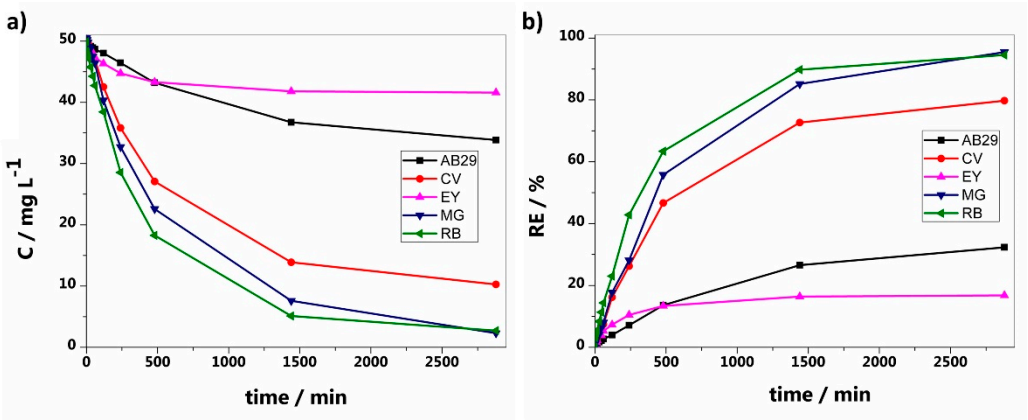

Figure 3. Adsorption curves of AB29, CV, EY, MG, and RB in terms of (a) initial concentration and (b) recovery percentage.

 doi:10.20944/preprints202504.1306.v1

Dye adsorption curves have been fitted assuming that adsorption process on GO-BP membranes could be described by Lagergren first-order kinetic model [34]:

$$\frac{dq_t}{dt} = k_1(q_e - q_t) \quad (3)$$

with q_t and q_e being respectively dye adsorption capacity per unit of adsorbent mass (mg·g^{-1}) at time t and at equilibrium (e) and k_1 is the Lagergren adsorption rate constant (min^{-1}). After integration, linearized form of Eq. 3 becomes (Eq. 4):

$$\ln(q_e - q_t) = \ln q_e - k_1 t \quad (4)$$

Lagergren adsorption rate constants and corresponding R^2 values are reported in Table 1. As corroborated by R^2 values, a first-order fitting suits properly the behavior observed experimentally, confirming that adsorption process is faster for MG (k_1 = 0.0017) and RB (k_1 = 0.0021), which also benefit from the highest adsorption values. Interestingly, despite its low recovery percentage, EY exhibits a kinetic constant quite similar to CV (k_1 = 0.0011 vs k_1 = 0.0013, respectively), indicating that EY adsorption process on GO-BP membranes is quick, so much so that equilibrium is achieved after only 240 min, while a five-fold time is required to the other dyes to reach the *plateau* region. This potential high value of EY kinetic constant should not mislead with GO-BP adsorption capacity for this dye. The latter indeed depends on the typology and quality of interactions between EY and GO-BP surface. On the other hand, the kinetic model studies the process in terms of rate of occupied sites. Therefore, this apparent contradiction inbetween kinetic constant and adsorption capacity values simply suggests that EY rapidly occupies adsorbent sites available on GO-BP surface until hydrophobic interactions prevail. Afterwards, due to their negative charges, increasing pollutant amount on GO-BP membrane exposes both involved parts to a notably electrostatic repulsion, which becomes predominantly and interrupts the addition of further pollutant on GO-BP surface.

Table 1. K_D, q_{max} and k values for AB29, CV, EY, MG and RB at: C_{dye} = 50 mg L^{-1}, pH=6, r.t.

Dye	LogK$_D$	Maximun adsorption capacity (mg g^{-1})	1st order kinetic constant (min^{-1})	R^2
AB29	3.58	129.31	0.0004 ± 0.0001	0.9906
CV	4.50	323.74	0.0013 ± 0.0004	0.9972
EY	3.21	67.09	0.0011 ± 0.0003	0.9776
MG	5.23	390.17	0.0017 ± 0.0004	0.9968
RB	5.14	377.53	0.0021 ± 0.0006	0.9974

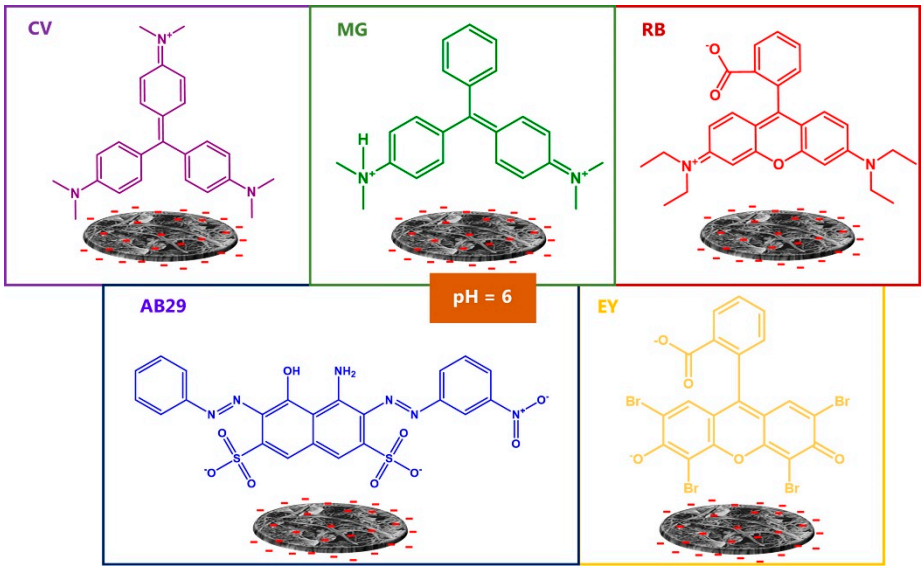

Figure 4. Schematic representation of electrostatic interactions establishing between GO-BPs and dyes molecules.

 doi:10.20944/preprints202504.1306.v1

In order to evaluate maximum adsorption capacity of GO-BP membranes, adsorption experiments were repeated at increased dye concentration of 100 mg L^{-1} each. Final values are reported in Table 2, attesting the high potentiality of GO-BP membranes towards RB (467 mg g^{-1}) and MG (493 mg g^{-1}), for which q_{max} rises of a further 25% when initial concentration moves from 50 to 100 mg L^{-1}.

Considering stability and efficiency over long-term use, GO-BP membranes were recycled and reused in successive adsorption tests, repeating experiments for each dye at 50 mg L^{-1} for five times. Regeneration step was performed by washing GO-BP membranes at the end of each adsorption cycle with an ethanol:water (2:1) solution for three times, and then drying GO-BPs at room temperature. With a discrepancy in RE% values of 4% at maximum between the first and last cycle, recycle experiments ascertained the reusability of GO-BP membranes for subsequent adsorption tests, maintaining their recovery percentages (Figure 5) towards dyes almost unchanged up to five times from the first experiment.

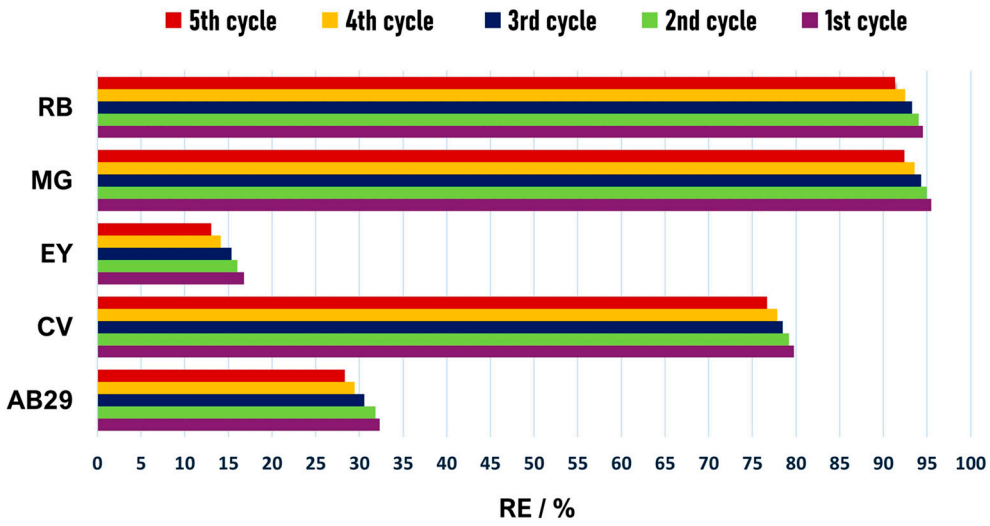

Figure 5. Recovery percentages of GO-BPs towards AB29, CV, EY, MG, and RB in 5 regeneration cycles (C_{AB29} = C_{CV} = C_{EY} = C_{MG} = C_{RB} = 50 mg L^{-1}).

3.1. Comparison with Other Adsorbents

To better comprehend the adsorption potential of GO-BP membranes towards dyes, a comparison of some literature data is proposed in Table 2. The table emphasizes the most relevant aspects to be considered when designing adsorption process, such as pH, amount of adsorbent, and dye initial concentration, also providing the q_{max} value associated to each cited work. Despite the authors intent to narrow the field only to references concerning the employment of GO, the scarcity or, in some cases, the lack of literature data about the adsorption of investigated dyes through GO forced them to expand the research and consider more adsorbents than only graphene oxide. Considering data presented in Table 2, it is evident that, where the comparison is possible, GO has an added value than some natural adsorbents, such kaolin, or rice husk, suggesting how fundamental is the contribute of GO large surface area to dyes adsorption. This is particularly evident in the case of AB29, where the use of GO-BP membranes enables to achieve a maximum adsorption capacity value three/four times higher than those reported in literature using a total adsorbent amount significantly lower (50 mg vs. 300/500 mg). A similar trend is observed for EY, where GO-BP membranes ensure a better adsorption capacity than some conventional adsorbents (zeolite Y). However, it is clearly evident that the difference is the pH. In acidic conditions, EY exhibits a less negative form which can electrostatically interact with GO positive surface, favoring adsorption. This can explain the high q_{max} values (217 and 555 mg g^{-1}, respectively) joined with GO by Veerakumar et al. [35], and Ahmad et al. [36], exceeding adsorption capacity results found in this work, where experiments were performed at pH=6. With their strong interactions with GO surface, CV, MB and

 doi:10.20944/preprints202504.1306.v1

RB are the favored substrates to be captured at pH=6. Confirming the behavior already observed for AB29, GO-BP membranes are able to efficiently retain large quantities of the above-mentioned dyes, exhibiting q_{max} values, at constant adsorbent amount, similar, or even upper, than those reported in literature. The possibility to entrap huge amounts of dyes by using low adsorbent contents marks the great potential of GO-BP membranes developed in this work as excellent adsorbents in dyes recovery.

Table 2. Comparison of maximum adsorption capacities of different adsorbents towards AB29, CV, EY, MG, and RB at room temperature.

Dye	Adsorbent typology	Adsorbent dose /(mg)	pH	C_{dye}/ (mg L^{-1})	C_{max} / (mg g^{-1})	Ref.
AB29	MgO-SiO_2	500	10	100	44.9	[37]
	K_2CO_3-activated olive pomace boiler ash	300	6	100	38.48	[38]
	GO-BP	50	6	100	162.65	This work
CV	Kaolin	100	7	100	45.0	[39]
	NaOH-modified rice husk	1000	7	50	44.87	[40]
	MWCNT-COOH	10	6	500	100.0	[41]
	GO	25	6	200	487.80	[42]
	GO-BP	50	6	100	374.53	This work
EY	Zeolite Y	100	2.5	60	52.91	[43]
	CNTs incorporated eucalyptus	20	6	50	49.15	[44]
	GO	300	1	50	217.33	[35]
	GO/ZnO nanocomposite	230	2	100	555.55	[36]
	GO-BP	50	6	100	85.38	This work
MG	Fe_3O_4-AC	100	6	300	217.68	[45]
	GO/aminated lignin aerogels	20	8	50	113.5	[46]
	GO-Cellulose-Cu	1000	7	400	207.1	[47]
	MWCNT-COOH	40	7	100	142.85	[48]
	rGO	50	7	200	476.2	[49]
	GO-BP	50	6	100	493.44	This work
RB	Magnesium silicate/carbon composite	100	6.5	600	244	[50]
	Montmorillonite/GO	300	7	150	625.0	[51]
	Benzene carboxylic acid/ GO-zeolite	10	3	500	67.56	[52]
	MWCNT-COOH	50	7	100	42.68	[53]
	GO-BP	50	6	100	467.35	This work

 doi:10.20944/preprints202504.1306.v1

5. Conclusions

In this work, an alternative version of CNTs buckypapers is proposed by GO incorporation into the inner structure of BPs. The obtained system (GO-BPs) takes advantage from both components combining GO properties, such large surface area and huge adsorption capacity, with BP specifics, including high mechanical and chemical stability, standing-alone property, and flexibility. The preparation of GO-BP membranes has the aim to propose GO-BPs as adsorbents in dyes removal from aqueous solutions. The authors selected five dyes (AB29, CV, EY, MG, and RB), differing for chemical structure and classification, and tested GO-BPs adsorption performance starting from C_i = 50 mg L^{-1} per dye (pH=6 and r. t.). Results pointed out that best adsorption performance are achieved when dye capture on GO-BP surface is promoted not only by hydrophobic interactions but also by electrostatic ones, the latters contributing dramatically to enhance the amount of retained dye. In view of this, maximum adsorption capacities have been observed for MG (493.44 mg g^{-1}) and RB (467.35 mg g^{-1}), followed by CV (374.53 mg g^{-1}), AB29 (162.65 mg g^{-1}) and EY (85.38 mg g^{-1}). In conclusion, GO-BPs appear a flexible, fast and sustainable solution for the efficient recovery of a large variety of dyes through adsorption processesThis section is not mandatory but can be added to the manuscript if the discussion is unusually long or complex.

Author Contributions: Conceptualization, M.B; data curation, M.B; formal analysis, M.B; funding acquisition, G. D. F.; investigation, M.B; methodology, M.B; project administration, G. D. F.; supervision, M.B, F. P. N. and G. D. F.; visualization, M.B; writing—original draft, M.B; writing—review & editing, M.B. F. P. N. and G. D. F. All authors have read and agreed to this version of the manuscript.

Funding: Author would like to offer specials thanks to MIUR, Italian Ministry for University and Research, grant number EX-60%/2025.

Conflicts of Interest: The authors declare no conflicts of interest.

Abbreviations

The following abbreviations are used in this manuscript:

SWCNT-BP	single-walled carbon nanotube buckypaper
MWCNTs	multi-walled carbon nanotubes
GO	graphene oxide
BP	buckypaper
AB29	acid blue 29
CV	crystal violet
EY	eosyn Y
MG	malachite green
RB	rhodamine B

References

1. United Nations Organization *The Sustainable Development Goals (SDGS)*; 2024;
2. Islam, T.; Repon, M.R.; Islam, T.; Sarwar, Z.; Rahman, M.M. *Impact of Textile Dyes on Health and Ecosystem: A Review of Structure, Causes, and Potential Solutions*; Springer Berlin Heidelberg, 2023; Vol. 30; ISBN 0123456789.
3. IMARC *Report Textile Market by Raw Material, Product, Application, and Region 2025-2033*; 2025;
4. Goswami, D.; Mukherjee, J.; Mondal, C.; Bhunia, B. Bioremediation of Azo Dye: A Review on Strategies, Toxicity Assessment, Mechanisms, Bottlenecks and Prospects. *Sci. Total Environ.* **2024**, *954*, 176426, doi:10.1016/j.scitotenv.2024.176426.
5. Berradi, M.; Hsissou, R.; Khudhair, M.; Assouag, M.; Cherkaoui, O.; El Bachiri, A.; El Harfi, A. Textile Finishing Dyes and Their Impact on Aquatic Environs. *Heliyon* **2019**, *5*, e02711, doi:10.1016/j.heliyon.2019.e02711.

 doi:10.20944/preprints202504.1306.v1

6. Al-Tohamy, R.; Ali, S.S.; Li, F.; Okasha, K.M.; Mahmoud, Y.A.G.; Elsamahy, T.; Jiao, H.; Fu, Y.; Sun, J. A Critical Review on the Treatment of Dye-Containing Wastewater: Ecotoxicological and Health Concerns of Textile Dyes and Possible Remediation Approaches for Environmental Safety. *Ecotoxicol. Environ. Saf.* **2022**, *231*, 113160, doi:10.1016/j.ecoenv.2021.113160.
7. Balakrishnan, V.K.; Shirin, S.; Aman, A.M.; de Solla, S.R.; Mathieu-Denoncourt, J.; Langlois, V.S. Genotoxic and Carcinogenic Products Arising from Reductive Transformations of the Azo Dye, Disperse Yellow 7. *Chemosphere* **2016**, *146*, 206–215, doi:10.1016/j.chemosphere.2015.11.119.
8. Solayman, H.M.; Hossen, M.A.; Abd Aziz, A.; Yahya, N.Y.; Leong, K.H.; Sim, L.C.; Monir, M.U.; Zoh, K.D. Performance Evaluation of Dye Wastewater Treatment Technologies: A Review. *J. Environ. Chem. Eng.* **2023**, *11*, 109610, doi:10.1016/j.jece.2023.109610.
9. Chethana, M.; Sorokhaibam, L.G.; Bhandari, V.M.; Raja, S.; Ranade, V. V. Green Approach to Dye Wastewater Treatment Using Biocoagulants. *ACS Sustain. Chem. Eng.* **2016**, *4*, 2495–2507, doi:10.1021/acssuschemeng.5b01553.
10. Bhatnagar, R.; Joshi, H.; Mall, I.D.; Srivastava, V.C. Electrochemical Treatment of Acrylic Dye-Bearing Textile Wastewater: Optimization of Operating Parameters. *Desalin. Water Treat.* **2014**, *52*, 111–122, doi:10.1080/19443994.2013.786653.
11. Fortunato, L.; Elcik, H.; Blankert, B.; Ghaffour, N.; Vrouwenvelder, J. Textile Dye Wastewater Treatment by Direct Contact Membrane Distillation: Membrane Performance and Detailed Fouling Analysis. *J. Memb. Sci.* **2021**, *636*, 119552, doi:10.1016/j.memsci.2021.119552.
12. Wong, J.K.H.; Tan, H.K.; Lau, S.Y.; Yap, P.S.; Danquah, M.K. Potential and Challenges of Enzyme Incorporated Nanotechnology in Dye Wastewater Treatment: A Review. *J. Environ. Chem. Eng.* **2019**, *7*, 103261, doi:10.1016/j.jece.2019.103261.
13. Rashid, R.; Shafiq, I.; Akhter, P.; Iqbal, M.J.; Hussain, M. A State-of-the-Art Review on Wastewater Treatment Techniques: The Effectiveness of Adsorption Method. *Environ. Sci. Pollut. Res.* **2021**, *28*, 9050–9066, doi:10.1007/s11356-021-12395-x.
14. Jia, J.; Wu, D.; Yu, J.; Gao, T.; Guo, L.; Li, F. Upgraded β-Cyclodextrin-Based Broad-Spectrum Adsorbents with Enhanced Antibacterial Property for High-Efficient Dyeing Wastewater Remediation. *J. Hazard. Mater.* **2024**, *461*, 132610, doi:10.1016/j.jhazmat.2023.132610.
15. Cai, Z.; Sun, Y.; Liu, W.; Pan, F.; Sun, P.; Fu, J. An Overview of Nanomaterials Applied for Removing Dyes from Wastewater. *Environ. Sci. Pollut. Res.* **2017**, *24*, 15882–15904, doi:10.1007/s11356-017-9003-8.
16. Baratta, M.; Nezhdanov, A.V.; Mashin, A.I.; Nicoletta, F.P.; De Filpo, G. Carbon Nanotubes Buckypapers: A New Frontier in Wastewater Treatment Technology. *Sci. Total Environ.* **2024**, *924*, 171578, doi:10.1016/j.scitotenv.2024.171578.
17. Umesh, A.S.; Puttaiahgowda, Y.M.; Thottathil, S. Enhanced Adsorption: Reviewing the Potential of Reinforcing Polymers and Hydrogels with Nanomaterials for Methylene Blue Dye Removal. *Surfaces and Interfaces* **2024**, *51*, 104670, doi:10.1016/j.surfin.2024.104670.
18. Thakur, A.; Kumar, A.; Singh, A. Adsorptive Removal of Heavy Metals, Dyes, and Pharmaceuticals: Carbon-Based Nanomaterials in Focus. *Carbon N. Y.* **2024**, *217*, 118621, doi:10.1016/j.carbon.2023.118621.
19. Baratta, M.; Tursi, A.; Curcio, M.; Cirillo, G.; Nezhdanov, A.V.; Mashin, A.I.; Nicoletta, F.P.; De Filpo, G. Removal of Non-Steroidal Anti-Inflammatory Drugs from Drinking Water Sources by GO-SWCNT Buckypapers. *Molecules* **2022**, *27*, 7674, doi:10.3390/molecules27227674.
20. De Filpo, G.; Pantuso, E.; Mashin, A.I.; Baratta, M.; Nicoletta, F.P. WO3/Buckypaper Membranes for Advanced Oxidation Processes. *Membranes (Basel).* **2020**, *10*, 1–16, doi:10.3390/membranes10070157.

 doi:10.20944/preprints202504.1306.v1

21. Baratta, M.; Nezhdanov, A.V.; Ershov, A.V.; Aiello, D.; Napoli, A.; Donna, L. Di; Mashin, A.I.; Nicoletta, F.P.; Filpo, G. De Improving the Catalytic Performance of TiO 2 by Its Surface Deposition on CNT Buckypapers for Use in the Removal of Wastewater Pollutants. *New Carbon Mater.* **2025**, *40*, 438–455, doi:10.1016/S1872-5805(25)60966-8.
22. Tursi, A.; Mastropietro, T.F.; Bruno, R.; Baratta, M.; Ferrando-Soria, J.; Mashin, A.I.; Nicoletta, F.P.; Pardo, E.; De Filpo, G.; Armentano, D. Synthesis and Enhanced Capture Properties of a New BioMOF@SWCNT-BP: Recovery of the Endangered Rare-Earth Elements from Aqueous Systems. *Adv. Mater. Interfaces* **2021**, *8*, 2100730, doi:10.1002/admi.202100730.
23. Baratta, M.; Mastropietro, T.F.; Bruno, R.; Tursi, A.; Negro, C.; Ferrando-Soria, J.; Mashin, A.I.; Nezhdanov, A.; Nicoletta, F.P.; De Filpo, G.; et al. Multivariate Metal-Organic Framework/Single-Walled Carbon Nanotube Buckypaper for Selective Lead Decontamination. *ACS Appl. Nano Mater.* **2022**, *5*, 5223–5233, doi:10.1021/acsanm.2c00280.
24. Baratta, M.; Mastropietro, T.F.; Escamilla, P.; Algieri, V.; Xu, F.; Nicoletta, F.P.; Ferrando-Soria, J.; Pardo, E.; De Filpo, G.; Armentano, D. Sulfur-Functionalized Single-Walled Carbon Nanotube Buckypaper/MTV-BioMetal-Organic Framework Nanocomposites for Gold Recovery. *Inorg. Chem.* **2024**, *63*, 18992−19001, doi:10.1021/acs.inorgchem.4c03407.
25. Baratta, M.; Tursi, A.; Curcio, M.; Cirillo, G.; Nicoletta, F.P.; De Filpo, G. GO-SWCNT Buckypapers as an Enhanced Technology for Water Decontamination from Lead. *Molecules* **2022**, *27*, 1–13, doi:10.3390/molecules27134044.
26. Chun, M.S.; Lee, S.Y.; Yang, S.M. Estimation of Zeta Potential by Electrokinetic Analysis of Ionic Fluid Flows through a Divergent Microchannel. *J. Colloid Interface Sci.* **2003**, *266*, 120–126, doi:10.1016/S0021-9797(03)00576-9.
27. Akrami, M.; Danesh, S.; Eftekhari, M. Comparative Study on the Removal of Cationic Dyes Using Different Graphene Oxide Forms. *J. Inorg. Organomet. Polym. Mater.* **2019**, *29*, 1785–1797, doi:10.1007/s10904-019-01140-0.
28. Bradder, P.; Ling, S.K.; Wang, S.; Liu, S. Dye Adsorption on Layered Graphite Oxide. *J. Chem. Eng. Data* **2011**, *56*, 138–141, doi:10.1021/je101049g.
29. Minitha, C.R.; Lalitha, M.; Jeyachandran, Y.L.; Senthilkumar, L.; Rajendra Kumar, R.T. Adsorption Behaviour of Reduced Graphene Oxide towards Cationic and Anionic Dyes: Co-Action of Electrostatic and $\pi - \pi$ Interactions. *Mater. Chem. Phys.* **2017**, *194*, 243–252, doi:10.1016/j.matchemphys.2017.03.048.
30. Konicki, W.; Aleksandrzak, M.; Mijowska, E. Equilibrium, Kinetic and Thermodynamic Studies on Adsorption of Cationic Dyes from Aqueous Solutions Using Graphene Oxide. *Chem. Eng. Res. Des.* **2017**, *123*, 35–49, doi:10.1016/j.cherd.2017.03.036.
31. Narayanaswamy, V.; Alaabed, S.; Al-Akhras, M.A.; Obaidat, I.M. Molecular Simulation of Adsorption of Methylene Blue and Rhodamine B on Graphene and Graphene Oxide for Water Purification. *Mater. Today Proc.* **2019**, *28*, 1078–1083, doi:10.1016/j.matpr.2020.01.086.
32. Ramesha, G.K.; Vijaya Kumara, A.; Muralidhara, H.B.; Sampath, S. Graphene and Graphene Oxide as Effective Adsorbents toward Anionic and Cationic Dyes. *J. Colloid Interface Sci.* **2011**, *361*, 270–277, doi:10.1016/j.jcis.2011.05.050.
33. Sedeño-Díaz, J.; Eugenia, L.; Mendoza-mart, E.; Joseph, A.; Soledad, S. Distribution Coefficient and Metal Pollution Index in Water and Sediments: Proposal of a New Index for Ecological Risk Assessment of Metals. *Water (Switzerland)* **2019**, *12*, 1–20, doi:doi:10.3390/w12010029.
34. Wang, J.; Guo, X. Adsorption Kinetic Models: Physical Meanings, Applications, and Solving Methods. *J. Hazard. Mater.* **2020**, *390*, 122156, doi:10.1016/j.jhazmat.2020.122156.

 doi:10.20944/preprints202504.1306.v1

35. Veerakumar, P.; Tharini, J.; Ramakrishnan, M.; Panneer Muthuselvam, I.; Lin, K.C. Graphene Oxide Nanosheets as An Efficient and Reusable Sorbents for Eosin Yellow Dye Removal from Aqueous Solutions. *ChemistrySelect* **2017**, *2*, 3598–3607, doi:10.1002/slct.201700281.
36. Ahmad, N.; Karim, S.; Hussain, D.; Mok, Y.S.; Siddiqui, G.U. Efficient Dual Adsorption of Eosin Y and Methylene Blue from Aqueous Solution Using Nanocomposite of Graphene Oxide Nanosheets and ZnO Nanospheres. *Korean J. Chem. Eng.* **2022**, *39*, 3155–3164, doi:10.1007/s11814-022-1164-6.
37. Ciesielczyk, F.; Bartczak, P.; Zdarta, J.; Jesionowski, T. Active MgO-SiO2 Hybrid Material for Organic Dye Removal: A Mechanism and Interaction Study of the Adsorption of C.I. Acid Blue 29 and C.I. Basic Blue 9. *J. Environ. Manage.* **2017**, *204*, 123–135, doi:10.1016/j.jenvman.2017.08.041.
38. Marrakchi, F.; Bouaziz, M.; Hameed, B.H. Adsorption of Acid Blue 29 and Methylene Blue on Mesoporous K2CO3-Activated Olive Pomace Boiler Ash. *Colloids Surfaces A Physicochem. Eng. Asp.* **2017**, *535*, 157–165, doi:10.1016/j.colsurfa.2017.09.014.
39. Nandi, B.K.; Goswami, A.; Das, A.K.; Mondal, B.; Purkait, M.K. Kinetic and Equilibrium Studies on the Adsorption of Crystal Violet Dye Using Kaolin as an Adsorbent. *Sep. Sci. Technol.* **2008**, *43*, 1382–1403, doi:10.1080/01496390701885331.
40. Chakraborty, S.; Chowdhury, S.; Das Saha, P. Adsorption of Crystal Violet from Aqueous Solution onto NaOH-Modified Rice Husk. *Carbohydr. Polym.* **2011**, *86*, 1533–1541, doi:10.1016/j.carbpol.2011.06.058.
41. Sabna, V.; Thampi, S.G.; Chandrakaran, S. Adsorption of Crystal Violet onto Functionalised Multi-Walled Carbon Nanotubes: Equilibrium and Kinetic Studies. *Ecotoxicol. Environ. Saf.* **2016**, *134*, 390–397, doi:10.1016/j.ecoenv.2015.09.018.
42. Puri, C.; Sumana, G. Highly Effective Adsorption of Crystal Violet Dye from Contaminated Water Using Graphene Oxide Intercalated Montmorillonite Nanocomposite. *Appl. Clay Sci.* **2018**, *166*, 102–112, doi:10.1016/j.clay.2018.09.012.
43. Adeoye, J.B.; Balogun, D.O.; Etemire, O.J.; Ezeh, P.N.; Tan, Y.H.; Mubarak, N.M. Rapid Adsorptive Removal of Eosin Yellow and Methyl Orange Using Zeolite Y. *Sci. Rep.* **2023**, *13*, 1–15, doi:10.1038/s41598-023-48675-4.
44. Yadav, S.K.; Dhakate, S.R.; Pratap Singh, B. Carbon Nanotube Incorporated Eucalyptus Derived Activated Carbon-Based Novel Adsorbent for Efficient Removal of Methylene Blue and Eosin Yellow Dyes. *Bioresour. Technol.* **2022**, *344*, 126231, doi:10.1016/j.biortech.2021.126231.
45. Altintig, E.; Onaran, M.; Sarı, A.; Altundag, H.; Tuzen, M. Preparation, Characterization and Evaluation of Bio-Based Magnetic Activated Carbon for Effective Adsorption of Malachite Green from Aqueous Solution. *Mater. Chem. Phys.* **2018**, *220*, 313–321, doi:10.1016/j.matchemphys.2018.05.077.
46. Chen, H.; Liu, T.; Meng, Y.; Cheng, Y.; Lu, J.; Wang, H. Novel Graphene Oxide/Aminated Lignin Aerogels for Enhanced Adsorption of Malachite Green in Wastewater. *Colloids Surfaces A Physicochem. Eng. Asp.* **2020**, *603*, 125281, doi:10.1016/j.colsurfa.2020.125281.
47. Khawaja, H.; Zahir, E.; Asghar, M.A.; Asghar, M.A. Graphene Oxide Decorated with Cellulose and Copper Nanoparticle as an Efficient Adsorbent for the Removal of Malachite Green. *Int. J. Biol. Macromol.* **2021**, *167*, 23–34, doi:10.1016/j.ijbiomac.2020.11.137.
48. Shirmardi, M.; Mahvi, A.H.; Hashemzadeh, B.; Naeimabadi, A.; Hassani, G.; Niri, M.V. The Adsorption of Malachite Green (MG) as a Cationic Dye onto Functionalized Multi Walled Carbon Nanotubes. *Korean J. Chem. Eng.* **2013**, *30*, 1603–1608, doi:10.1007/s11814-013-0080-1.
49. Gupta, K.; Khatri, O.P. Reduced Graphene Oxide as an Effective Adsorbent for Removal of Malachite Green Dye: Plausible Adsorption Pathways. *J. Colloid Interface Sci.* **2017**, *501*, 11–21, doi:10.1016/j.jcis.2017.04.035.

 doi:10.20944/preprints202504.1306.v1

50. Sun, Z.; Duan, X.; Srinivasakannan, C.; Liang, J. Preparation of Magnesium Silicate/Carbon Composite for Adsorption of Rhodamine B. *RSC Adv.* **2018**, *8*, 7873–7882, doi:10.1039/c7ra12848g.
51. Neelaveni, M.; Santhana Krishnan, P.; Ramya, R.; Sonia Theres, G.; Shanthi, K. Montmorillonite/Graphene Oxide Nanocomposite as Superior Adsorbent for the Adsorption of Rhodamine B and Nickel Ion in Binary System. *Adv. Powder Technol.* **2019**, *30*, 596–609, doi:10.1016/j.apt.2018.12.005.
52. Yu, Y.; Murthy, B.N.; Shapter, J.G.; Constantopoulos, K.T.; Voelcker, N.H.; Ellis, A. V. Benzene Carboxylic Acid Derivatized Graphene Oxide Nanosheets on Natural Zeolites as Effective Adsorbents for Cationic Dye Removal. *J. Hazard. Mater.* **2013**, *260*, 330–338, doi:10.1016/j.jhazmat.2013.05.041.
53. Oyetade, O.A.; Nyamori, V.O.; Martincigh, B.S.; Jonnalagadda, S.B. Effectiveness of Carbon Nanotube-Cobalt Ferrite Nanocomposites for the Adsorption of Rhodamine B from Aqueous Solutions. *RSC Adv.* **2015**, *5*, 22724–22739, doi:10.1039/c4ra15446k.